VISCOELASTICITY AND CREEP RECOVERY OF POLYIMIDE THIN FILMS

Fariborz Maseeh and Stephen D. Senturia
Microsystems Technology Laboratories
Massachusetts Institute of Technology, Cambridge, MA 02139

ABSTRACT

Creep and recovery of a polyimide thin film well below its glass transition temperature is demonstrated through use of circular membrane bulge test. Extensive use is made of a recently developed mechanical CAD system linked to the fabrication process to model the structure. A creep power law is used in a nonlinear finite element (FEM) analysis to fit the experimental results, thereby measuring the viscoelastic properties.

INTRODUCTION

Recently, polyimide films have been used as structural components of mechanical microsensors and microactuators [1-3]. Polyimides, like most polymers, exhibit a time dependent mechanical response (viscoelasticity). This is potentially an important factor in the design of mechanical structures in which polyimide is subjected to sustained loads.

Viscoelastic properties of materials are traditionally measured by uniaxial tests [4]. Creep, stress-relaxation, and dynamic-loading tests are the commonly used techniques to measure the time-dependent analogs to elastic constants. The uniaxial creep test consists of measuring the time-dependent stretch resulting from the application of a steady axial load, and can be directly related to the viscoelastic properties. Uniaxial experiments, though effective for large samples, can be difficult to implement for thin films. We employ circular membranes to perform a biaxial creep experiment in which a time-dependent deformation is measured under a state of biaxial stress. This technique eliminates the sample handling problems and offers a way to detect and measure the viscoelastic behavior of the material. The membrane data, in the form of deflection as a function of applied pressure, need further modeling to extract the time dependent stress vs strain results. In this work, we report on creep and creep recovery of Dupont's commercial polyimide PI2525, and present a non-linear viscoelastic model for the interpretation of the creep behavior.

SAMPLE FABRICATION AND MEASUREMENTS

The PI2525 polyimide is the imidized form of the polyamic acid precursor that results from the reaction of benzophenone-tetracarboxylic dianhydride (BTDA) with a blend of meta-phenylenediamine (MPDA-40%) and oxydianiline (ODA-60%) [5]. The polyamic acid is supplied commercially dissolved in N-methylpyrollidone and is spin-cast, then cured to produce the polyimide. Circular polyimide membranes one inch in diameter and 5 μm in thickness are microfabricated using the technique described in [6]. The PI2525 precursor is spin deposited on (100) silicon substrates in multiple layers, prebaked at 130°C for 15 minutes after each layer for solvent removal and partial imidization, and then cured (imidized) at 400°C in nitrogen for one hour. A VESPEL ring, one inch in inner diameter, 1-1/8 inch in outside diameter, and 1/16 inch thick, is mounted on the polyimide side with epoxy, and the substrate is removed by chemical etching with an nitric-hydroflouric acid solution. The ring, which is sufficiently large to be considered rigid, captures the state of biaxial stress in the film at the support. The sample is mounted in our bulge test apparatus and the center deflection as a function of the applied pressure is measured by tracking the focus point using a digital micrometer attached to a microscope stage. The applied air pressure is measured by a Kulite LQ-5-516 pressure sensor calibrated for the working pressure ranges (0 - 0.1 MPa).

Fig. 1 shows the center deflection vs pressure for a PI2525 membrane. The portion of the curve below the point indicated by the arrow is elastic. Data from this portion of the curve are used to extract the residual stress and biaxial modulus of the film, as explained in [6]. For pressures above this point, the center displacement increases with time at fixed pressure. In this particular figure, the pressure is gradually increased until the deflection reached 2200 μm, after which the increase in deflection is monitored as a function of time. In actual creep experiments, the pressure load is increased at small intervals and the deflection is observed over a time scale of 2 minutes. If a time-dependent deformation is observed, indicating the threshold of observable creep (on the time scale of tens of seconds), the pressure is then increased to a fixed value well above the creep threshold, and the center deformation as a function of time is measured. Fig. 2 shows typical creep data, plotted as creep deflection d_{cr} vs time (the model is explained later). The creep deflection is defined as $d - d_s$ in Figure 1. The creep measurement continues until the center deflection stops changing on a time scale of 10 minutes. The sample is then unloaded and a plastically deformed dome shape surrounded by an elastic ring is observed shown schematically in Fig. 3. The width of the undeformed rim of the film is measured immediately after the unloading. This width is used in conjunction with elastic models of membrane deformation to estimate the strain at which creep initiates. After unloading, the polyimide sample gradually recovers its original flat shape. Fig. 4 shows a sequence of photographs for a PI2525 sample after unloading. The apparent total recovery time is 130 hours. After the recovery, a second load-deflection measurement is made in the elastic region. The biaxial modulus extracted from the second run agrees with the first run; however, the residual stress shows a 40% drop in value as a result of having cycled through the creep and creep-recovery sequence.

CH2783-9/90/0000-0055$01.00©1990 IEEE

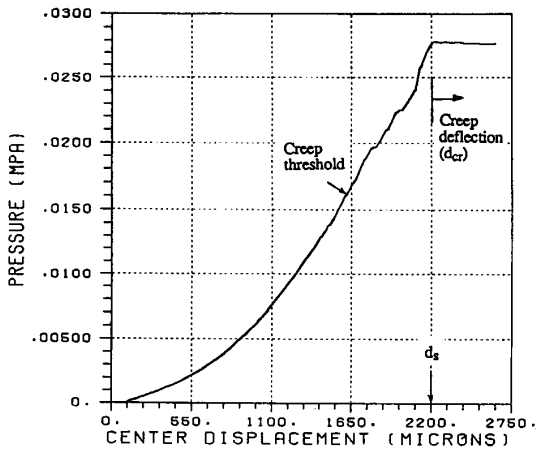

Fig. 1. Measured center deflection of a PI2525 circular membrane, one inch in diameter. The flat part is the viscoelastic deformation under constant pressure as a function of time.

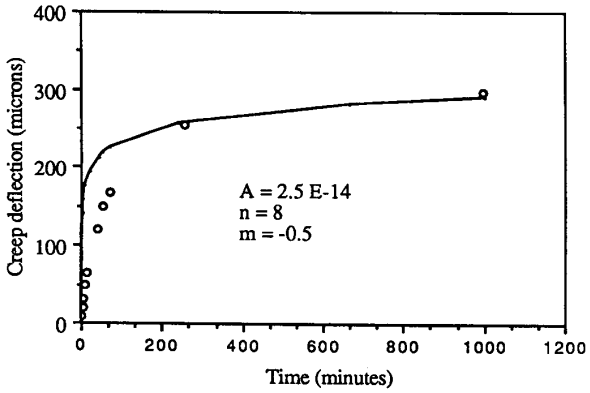

Fig. 2. FEM model of creep deflection vs time. Hollow circles are the measured data

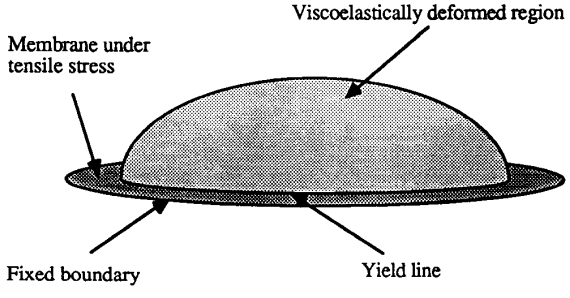

Fig. 3. PI2525 circular membrane viscoelastically deformed when unloaded. The deformed region recovers in time well below glass transition tempertaure.

DATA ANALYSIS

A. Modeling of the structure

The membrane fabrication and analysis is implemented in the environment of a previously reported CAD architecture [7,8], which uses a Structure Simulator supported by process modeling programs to create the solid model. The process modeling for spinning polyimide on a substrate uses data on film thickness vs spin speed for this particular polyimide [9] to generate a model for thickness (t_f in μm) as a function of spin speed (V_s in krpm) and the number of coats n. In the case of PI2525, a good representation of the data is provided by the expression $t_f = n\,[1/6 + 40/3V_s]$. A PFR (process flow representation [10]) of the polyimide deposition (including spinning, prebake, and cure steps) is developed. The Structure Simulator interprets the PFR process step description, determines the film thickness, and generates the solid model in a format which is directly readable by the mechanical modeling graphics pre/post processor PATRAN. Because of the radial symmetry of the samples, only two-dimensional models are generated. Within the PATRAN preprocessor graphics, the ring supporting the film is modeled by enforcing built-in conditions on the face of the film at the ring-film contact surface. The elastic properties (measured Young's modulus and Poisson's ratio from [6]) of polyimide (assumed isotropic) are loaded from a PATRAN-readable material property database file. Loads and boundary conditions and element types are specified. An ABAQUS input file is then generated assuming zero residual stress, and is modified manually to account for the residual stress in the polyimide. The viscoelastic properties are also entered by manual modification of the ABAQUS input file. The resulting model is sent to ABAQUS version 4-7 [11,12]; the analysis results are returned to PATRAN and are displayed graphically. The process modeling and FEM model generation are done on a SUN-4. The FEM simulations are done on both SUN-4 and the MIT-CRAY2 facility; in the latter case the ABAQUS output is transported back to SUN-4 for evaluation.

Since both the geometry and applied loads are axially symmetric, a two dimensional analysis is sufficient by taking a section through the thickness and a radius. 8-noded axisymmetric elements are used throughout the analysis. The suspended part of the film within the ring is modeled with 50 elements with element sizes linearly decreasing toward the edge to one-tenth of the one at the center, shown schematically in Fig. 5. The portion of the film adhering to the ring is modeled with 10 uniform elements fixed at the bottom edge as shown.

B. Analysis of viscoelastic behavior

For deformations in the elastic regime, the state of the stress in the loaded membrane is shown in Fig. 6. As shown, an unequal state of biaxial stress develops when the membrane is subjected to uniform lateral pressure. The nonuniform stress distribution in the membrane requires a more complex analysis to determine the viscoelastic properties of the film than when the uniaxial measurement is used. Under the condition of the uniaxial loading, the commonly adopted creep law is of the form:

$$v_{cr} = A\, q^n\, t^m \qquad (1)$$

where v_{cr} is the creep strain rate, q is the von Mises stress (a condition among the stress components at a point that must be satisfied for the onset of plastic deformation, in the case of simple tension: $2q^2 = [\sigma_1 - \sigma_2]^2 + [\sigma_2 - \sigma_3]^2 + [\sigma_1 - \sigma_3]^2$ where σ_i's are the principal stresses), A is a constant, n is a material dependent integer normally between 3 and 8 [13], and m is a (time hardening) constant between -1 and 0. All constants are to be determined by fitting to the creep measurement data. A modified creep law is used in this work by replacing q with $q-q_y$ where q_y is the creep threshold, the stress below which the material creep is negligible. The creep strain ε_{cr} is then determined by integrating eqn. (1) in time which results in:

$$\varepsilon_{cr} = [A/(m+1)]\,(q-q_y)^n\, t^{m+1} \qquad q > q_y$$
$$\varepsilon_{cr} = 0 \qquad q < q_y \qquad (2)$$

This results in creep when the stress is above the threshold stress (assumed to be 95 MPa for PI2525 from experimental observations). Eqn. (2) is incorporated in the FEM model. Investigation of this model reveals a linear relationship between the creep strain ε_{cr} and the creep deflection d_{cr} for different choices of the constants A, n, and m in the ranges of the measured displacements. Fig. 7 shows this relationship as obtained from FEM analysis. This result is used to determine the time-hardening exponent m directly from a fit to the measured d_{cr} vs t. This value is then utilized to extract values of A and n by a fit to the experimental results.

To extract the creep compliance from the experimental results, an iterative FEM procedure is utilized. The initial (order of magnitude) estimate of A is based on assuming linear viscoelasticity (n=1) and calculating the creep strains from an elastic deflection model [14,15]:

$$\varepsilon_{cr} = .67\,(d/a)^2 - .67\,(d_s/a)^2 \qquad (3)$$

where d is the total deflection, d_s the static deflection and a the membrane radius. Using this approximation, a value for A is extracted from a logarithmic fit to the ε_{cr} vs t curve. Then, with estimates of A and n (assumed unity in the first iteration) inserted into the FEM model, calculate the time-dependent deformation at the experimentally determined pressure (which at zero time yields the elastic deflection d_s), compare with experiment, and revise A and n until satisfactory convergence is achieved. In this case, no rigorous best fit is obtained, and error bounds on the resulting parameters can only be estimated. However, this procedure yields a reasonable approximation to the experimental data.

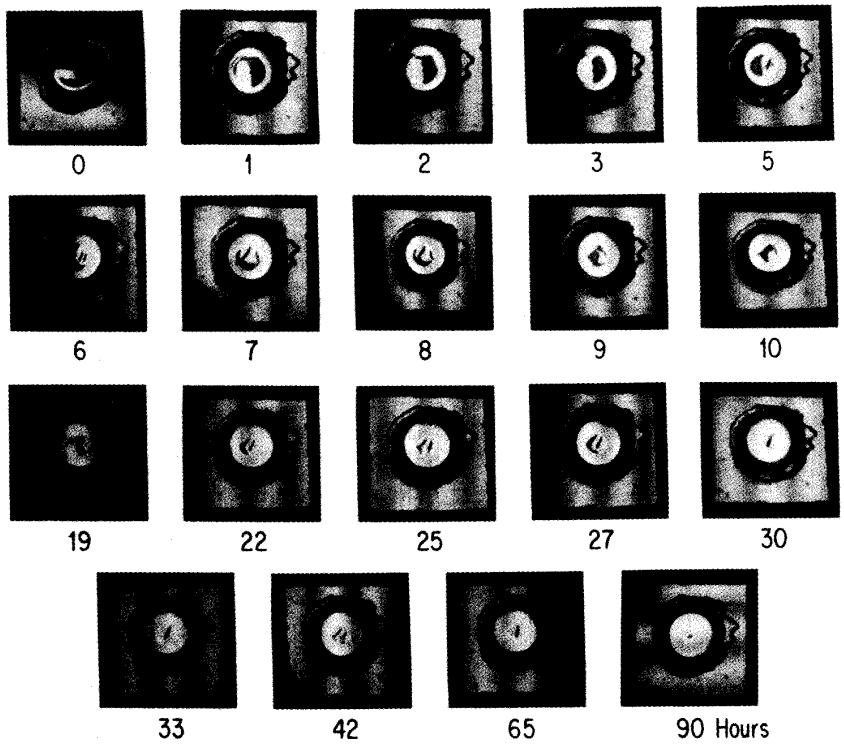

Fig. 4. Creep recovery of BTDA-MPDA/ODA polyimide (PI2525) at room temperature, when sample is unloaded. The glass transition temperature for this polyimide is above 300°C. The numbers below each photograph indicate the elapsed time in hours.

C. Results

The membrane pressure vs center deflection data consists of an elastic and a viscoelastic region. The elastic portion is used to determine the elastic properties of the thin film with the procedure in [6].

Fig. 6 shows the distribution of strains and stresses from the FEM in the meridian and the circumferential principal directions. The state of strain along the meridian (principal) direction in the deformed shape remains fairly constant along the radius; however the circumferential (principal) strain distribution is equal to the meridian one at the membrane center and decreases to zero at the support. These distributions are in agreement with a generalized membrane model [14,15], but deviate significantly from the Beam's spherical cap assumption [16]. The stress distribution along the meridian and circumferential directions behave as shown in Fig. 6, in agreement with the plane stress constitutive relation. The shear stresses are negligible. The maximum Mises stresses (and therefore plastic flow) occurs at the center of the membrane and gradually decrease toward the support as in the experiment. The center element is under the state of equal biaxial stress; therefore, this element is used throughout the analysis to characterize the viscoelastic properties.

Fig. 2 shows the FEM creep deflection vs time (for the center element) compared with the experimental results. The agreement is not perfect, but key features are well represented. Fig. 8, shows the resulting center element biaxial creep strain as a function of time. The biaxial creep strain ε_{bcr} is related to the uniaxial creep strain ε_{ucr} by the relation [17]:

$$\varepsilon_{bcr} = \varepsilon_{ucr} / 2 + \sigma / 6K \qquad (4)$$

where σ is the stress and K is the bulk modulus. Fig. 8 also shows the resulting uniaxial creep strain vs time.

The strain energy loss due to stress reduction in the film after recovery is related to the deviatoric (distortional) portion of the strain energy and is estimated form the expression [18]:

$$\Delta U_d = (1/6G) [\sigma_i^2 - \sigma_f^2] \qquad (5)$$

where G is the shear modulus, and σ_i and σ_f are the in-plane stresses, in the unloaded state, before and after the recovery. This energy loss (0.098 MJ/m^3) may be attributed to dissipation during the molecular distortions of the polymer chains during the creep. The effects of elevated temperature anneals on this energy loss has not been investigated, but would be interesting.

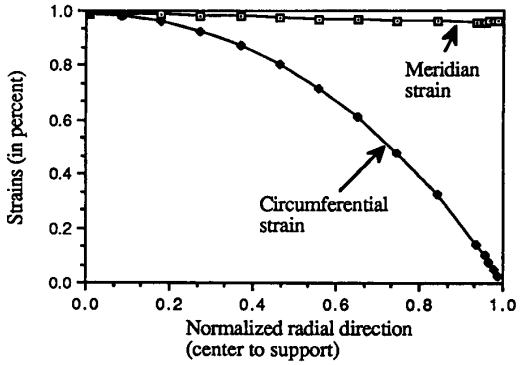

Fig. 6a. FEM meridian and circumferential strains for one inch circular PI2525 membrane

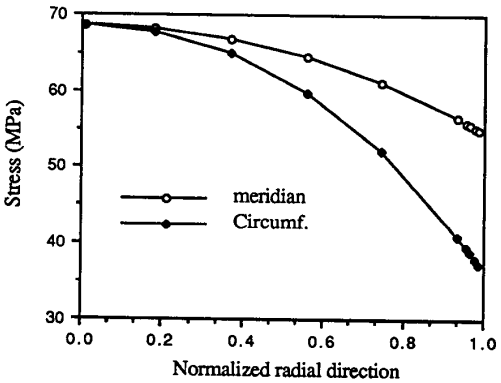

Fig. 6b. FEM Meridian and circumferential principal stresses for a circular PI2525 membrane

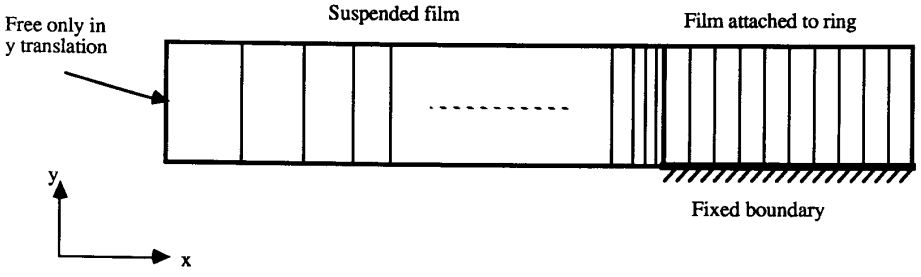

Fig. 5. Schematic finite element mesh for polyimide circular membranes. Axisymmetric elements (50 for suspended part and 10 for the fixed portion of the film) are used. Elements in the suspended film decrease uniformly from center to edge with a 10 to 1 ratio as shown.

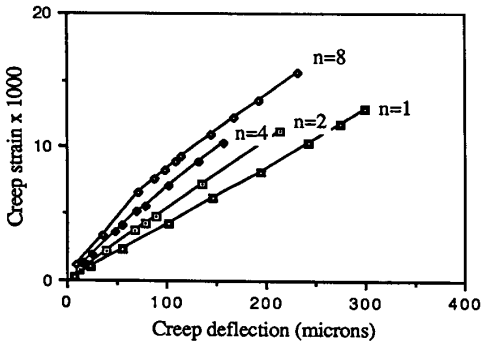

Fig. 7. Creep deflection vs biaxial strain in the center element (FEM model of PI2525 membrane)

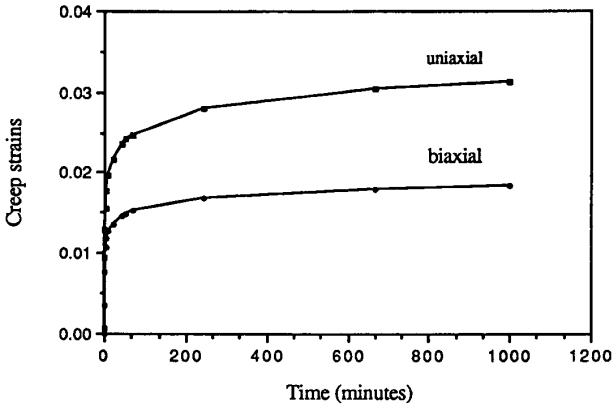

Fig. 8. Creep strains from a FEM vs time; the uniaxial strain is obtained from eqn (4)

CREEP RECOVERY

The creep recovery phenomenon illustrated in Figure 4 (shape memory effect) has been observed in polymers that are plastically deformed below their T_g when they are thermally loaded near or above their T_g; see e.g. [19,20]. In the experiment reported here, the polyimide is exhibiting creep recovery about 300 °C below its glass transition. Below the glass transition temperature, a polymer material must overcome two distinct sources of resistance before inelastic flow may occur [21,22]: (1) the material must be stressed above its intermolecular resistance to segment rotation (restrictions imposed on molecular chain motion by the neighboring chains), and (2) once the material begins to flow, molecular alignment occurs, altering the configurational entropy of the material. This entropy change, by analogy to the rubbery regime, may be related to the evolution of back stresses which can result in the recovery of the polymer [23]. The energy loss after shape recovery may be attributed to dissipating effects during reorientation of the polyimide chains.

Quantitative modeling of the recovery phenomenon will be reported elsewhere. The yield line for the recovering portion does not remain circular, and the contour for the deformed region is not easily measured without film disturbance. Qualitatively, it is observed that the recovery is temperature dependent. The sample recovers faster when the temperature is elevated. Humidity effects have not been investigated.

CONCLUSION

The use of circular membranes in measuring the viscoelastic and plastic material properties of thin films has some advantages over the uniaxial techniques. The membranes are edge free and therefore less susceptible to cracks which can prohibit observation of yield in glassy materials such as PI2525. The maximum stress region (center point) is also identified in advance; hence the viscoelastic properties of thin films can be observed without having to yield or creep the entire sample. However, the analysis to determine the viscoelastic properties is more cumbersome. This paper has presented a first attempt at such data analysis, and has determined that the creep compliance of PI2525 is a very nonlinear function of the stress (n = 8), and also requires a threshold strain before creep begins.

ACKNOWLEDGEMENTS

The authors wish to gratefully acknowledge Profs. Ali S. Argon, and David M. Parks of Mechanical Engineering Dept., Profs. Jerome J. Connor, and Shyam Sunder of Civil Engineering Dept. at MIT for their many technical remarks. We thank Duane S. Boning for the polyimide deposition PFR, and R. M. Harris for the structure simulator solid models. We extend our gratitude to HKS Inc. for the ABAQUS academic license and technical support, and to the MIT Super Computing Facilities for providing assistance for CRAY2 usage. This work was supported in part by Defence Advanced Research Program Agency under contract no. MDA972-88-k-0008. Microfabrication was carried out in the Microsystems Technology Laboratories of the MIT center for Material Science and Engineering, which is supported in part by the National Science Foundation under Contract No. DMR-87-19217.

REFERENCES

[1] M. A. Schmidt, R. T. Howe, S. D. Senturia, and J. H. Haritonidis, "Design and calibration of a microfabricated floating element shear-stress sensor", IEEE Trans. Elec. Dev., v. 35, June 1988, p. 750.

[2] M. G. Allen, M. Scheidl, R. L. Smith," Design and fabrication of movable silicon plates suspended by flexible supports", Proceedings of IEEE Micro Electro Mechanical Systems, Salt Lake City , Utah, Feb. 1989, p.76.

[3] M. Mehregany, R. Mahadevan, and K. J. Gabriel, "Application of electric microactuators to silicon micromechanics", Proceedings of Transducers'89, June 1989, Montreux, Switzerland.

[4] R. Mohan and D. F. Adams, "Nonlinear creep-recovery response of a polymer matrix and its composites", Exp. Mech., Sept. 1985, p. 262.

[5] P. V. Nagarkar, percentages from an XPS study, to be published.

[6] F. Maseeh, and S. D. Senturia,"Elastic properties of polyimide thin films", Polyimides ; Materials, Chemistry and Characterization, ed. by C. Feger, M. M. Khojasteh and J. E. Grath, Elsevier, Amsterdam, 1989, p. 575.

[7] F. Maseeh, R. M. Harris, and S. D. Senturia,"A CAD architecture for microelectromechanical design", Proceedings of IEEE Micro Electro Mechanical Systems, Napa Valley, CA, Feb. 1990, p. 44.

[8] R. M. Harris, F. Maseeh, and S. D. Senturia, "Automatic generation of a 3-D solid model of a microfabricated structure", Proceedings of this conference.

[9] D. Volfson, private communications.

[10] D. S. Boning, private communication.

[11] H. D. Hibbitt, "ABAQUS/EPGEN, a general purpose finite element code with emphasis on nonlinear applications", Nuc. Eng. Des., vol. 77, 1984, p. 271.

[12] ABAQUS User Manual, Release 4-7, HKS, Providence, RI.

[13] A.R. S. Ponter, and F. A. Leckie, "The application of energy theorems to bodies which creep in the plastic range", J. Appl. Mech. Sept. 1970, p. 753.

[14] A. E. Green, and J. E. Adkins, Large elastic deformations, Clarendon press, Oxford, 1970, p.133.

[15] T. Tsakalakos, "A comparison of theory and experiment for isotropic and anisotropic films", Thin solid films, v. 75, 1981, p. 293.

[16] J. W. Beams, "Mechanical properties of thin films of gold and silver", in C. A. Neugebauer, J. B. Newkirk, and D. A. Vermilyea, ed., Structure and Properties of Thin Films, Wiley & Sons, New York, 1959, p. 183.

[17] L. E. Nielsen, Mechanical properties of polymers and composites, v. 1, Marcel Dekker, Inc., NY, 1974, p.121.

[18] E. F. Byars, R. D. Snyder, and H. L. Plants, Engineering mechanics of deformable bodies, Fourth ed., Harper & Row, 1983, p. 417.

[19] Y. P. Khanna, R. Kumar, and A. C. Reimschuessel, "Memory effects in polymers III. Process history vs crystallization rate of Nylon 6-comments on the origin of memory effect", Pol. Eng. & Sc., v. 28, No. 24, 1988, p. 1607.

[20] A. Charlesby, and B. Kidric, "Memory effect in irradiated polymers", Radiat. Phys. Chem., v. 30, No. 1, 1987, p. 67.

[21] A. S. Argon, "A theory for the low-temperature plastic deformation of glassy polymers", Phil. Mag., vol. 28, 1973, p. 39.

[22] R. N. Howard, and G. Thackray, "The use of a mathematical model to describe isothermal stress-strain curves in glassy thermoplastics", Proc. Royal Soc. vol. 302, 1968, p. 453.

[23] M. C. Boyce, D. M. Parks, and A. S. Argon, "Large inelastic deformation of glassy polymers. Part I: rate dependent constitutive model", Mech. Mat., vol. 7, 1988, p. 15.